BJR

https://doi.org/10.1259/bjr.20190787

Received: 13 September 2019 | Revised: 18 November 2019 | Accepted: 28 November 2019

Cite this article as:
Parodi K. Latest developments in in-vivo imaging for proton therapy. *Br J Radiol* 2020; **93**: 20190787.

PROTON THERAPY SPECIAL FEATURE: REVIEW ARTICLE

Latest developments in in-vivo imaging for proton therapy

KATIA PARODI, PhD

Department of Experimental Physics – Medical Physics, Ludwig-Maximilians-Universität München, Faculty of Physics, Munich, Germany

Address correspondence to: Katia Parodi
E-mail: *katia.parodi@lmu.de*

ABSTRACT

Owing to the favorable physical and biological properties of swift ions in matter, their application to radiation therapy for highly selective cancer treatment is rapidly spreading worldwide. To date, over 90 ion therapy facilities are operational, predominantly with proton beams, and about the same amount is under construction or planning.
Over the last decades, considerable developments have been achieved in accelerator technology, beam delivery and medical physics to enhance conformation of the dose delivery to complex shaped tumor volumes, with excellent sparing of surrounding normal tissue and critical organs. Nevertheless, full clinical exploitation of the ion beam advantages is still challenged, especially by uncertainties in the knowledge of the beam range in the actual patient anatomy during the fractionated course of treatment, thus calling for continued multidisciplinary research in this rapidly emerging field. This contribution will review latest developments aiming to image the patient with the same beam quality as for therapy prior to treatment, and to visualize *in-vivo* the treatment delivery by exploiting irradiation-induced physical emissions, with different level of maturity from proof-of-concept studies in phantoms and first *in-silico* studies up to clinical testing and initial clinical evaluation.

INTRODUCTION

The characteristic dose maximum of proton beams at their end of range, so-called Bragg peak, opens several opportunities for a very precise dose delivery to the tumor, with superior sparing of normal tissue and organs at risk in comparison to the more widely used photon radiation.[1,2] These intrinsic physical advantages can be especially exploited in combination with the more recent technological advances of pencil beam scanning (PBS) delivery[3] and intensity modulated proton therapy (IMPT) treatment planning.[4] However, full clinical exploitation of these advantages in clinical practice is still challenged by remaining uncertainties in the knowledge of the daily (and even intrafractionally varying) patient anatomy and its stopping power properties. This calls for possibilities of getting updated volumetric patient model information at the treatment isocenter shortly before treatment, complemented by means of verifying the treatment delivery and, possibly, reconstructing the applied dose during or shortly after treatment.

In terms of patient model information for treatment planning, a need specific to ion beam therapy is the accurate description of the tissue stopping power ratio (SPR, relative to water) for relating the well-characterized ion range in water to the one in tissue, besides a realistic representation of the volumetric (possibly also time-resolved) patient anatomy. To this end, the well-established conversion of conventional single-energy X-ray Computed Tomography (CT) images into SPR via semi-empirical stoichiometric calibrations is introducing the likely largest source of uncertainties in the planned treatment range, reaching up to 3% or even more.[5] Solutions for improved and patient-specific SPR determination based on X-ray acquisitions at different energy spectra, as offered by commercially available dual-energy CT (DECT), have been extensively investigated in the last few years and are already finding their ways into the proton therapy clinical practice with very promising results.[6,7] However, alternatives under research and development based on the same radiation quality as for treatment offer the intriguing perspectives of a lower dose for daily image guidance at the treatment isocenter, with potentially even better SPR accuracy either from the combination of radiographic proton transmission imaging with volumetric X-ray CT, or directly from volumetric proton CT (pCT) imaging.[8] These pre-treatment methods could then be complemented by *in-vivo* verification of the ion range in tissue, exploiting the detection of physical irradiation-induced secondary emissions emerging from the patient

during or after treatment. In particular, the most widely investigated methods in the context of proton therapy exploit energetic γ radiation resulting from nuclear reaction radioactive products (yielding positron emissions with subsequent annihilation) and fast de-excitation radiative processes. This contribution reviews the status of development, initial clinical experience and prospects of such modalities, featuring proton transmission imaging as well as positron emission tomography (PET) and prompt γ (PG) imaging.

PROTON TRANSMISSION IMAGING

The usage of energetic ion beams able to traverse the patient had been proposed since the 1960s to provide radiographic images at higher density resolution than X-rays for tumor localization and position verification.[9–11] With the wider adoption of proton therapy in the 1990s, it was soon recognized that ion transmission imaging can provide pre-treatment patient-specific integral stopping power information for refinement of the CT-SPR calibration curve (radiography[12]), or direct reconstruction of three-dimensional (3D) SPR maps for usage in treatment planning (tomography[13]). In fact, the physical quantity of interest for ion therapy treatment (re)planning, namely the SPR, is in first approximation independent of the ion energy and even ion species. Hence, transmission images acquired at higher energies than for therapy, in order to place the Bragg peak in a detector outside the patient, can still be used for planning the treatment at the lower therapeutic energies, needed to place the Bragg peak in the tumor. However, the complexity and limited availability of rotating ion beam deliveries of sufficiently high energy for traversing the patient, along with the demands on the detection and data acquisition system, considerably slowed down the developments of this intriguing imaging modality. More recently, the topic has regained vivid interest worldwide, and different detector technologies are currently under investigation,[8,14] including a first prototype developed by a small start-up company (ProtonVDA, *www.protonvda.com*). In fact, the maximum proton beam energies of 230 MeV, corresponding to ca. 30 cm penetration depth in water, delivered by state-of-the-art gantry-equipped proton therapy facilities are deemed sufficient to image a large amount of anatomical locations of interest, especially in the cranial and upper abdomen regions.[15] Moreover, new proton therapy systems have recently become commercially available, which are designed to accelerate protons up to 330 MeV, corresponding to 60 cm penetration in water, for imaging purposes (*e.g.* by ProTom International, *www.protom-international.com*). All these facilities can provide large irradiation areas, either relying on passively scattered (broad-beam or cone-beam configuration) or actively scanned ion beams.

In terms of detector technologies, the most typical configurations aim at completely stopping the transmitted protons to determine their residual range or energy after traversing the imaging object. This can be accomplished by measuring either the proton stopping positions in a range telescope, *i.e.* a stack of detector channels like scintillation plates[16] or position-sensitive solid-state sensors,[17] or their residual energy deposited in a single or multistage calorimeter made of plastic scintillators[18] or inorganic crystals.[19] In case of a limited dynamic range of the detector, like for the above-mentioned first commercial prototype, additional absorbers may be introduced in the beam path to compensate for too thin areas of the sample to be traversed (however, requiring prior information of the imaged object). To overcome unavoidable limitations from multiple Coulomb scattering in the patient and air, the most advanced detector technologies combine the residual range/energy information of each individual proton with its trajectory along the object, estimated from a measurement of the entrance and exit beam coordinates (and even directions) in tracking planes in front and behind the imaging object. To this end, technologies investigated so far feature position sensitive scintillating fiber hodoscopes,[16] silicon strip detectors[13] or gas-based solutions.[20] With proper energy and angular cuts, post-processing techniques can further help eliminating unwanted events resulting from nuclear interactions or too large angle scattering, thus reducing the uncertainties in the recovered SPR values. However, such single particle detection systems also pose several challenges in terms of high costs and the required ability to handle event rates in the MHz range. Alternative cost-effective approaches exploit the integral signal produced from the entire beam. In case of broad fields with passive energy modulation, systems investigated so far include thin position sensitive detectors such as scintillation screens read out by cameras[21] and two-dimensional diode arrays.[22] For active beam scanning, the integrated Bragg curve of initially monoenergetic beams can be captured by multilayer dosimetric systems, such as stacks of large-area plane-parallel ionization chambers interleaved with passive absorbers.[23,24] However, despite their promising results, these integration mode setups typically suffer from degraded imaging performance in comparison to single particle tracking solutions, due to the issue of scattering in the object and range mixing effects in the integrated signal, calling for sophisticated data processing techniques and prior information. A comparison of these different imaging approaches and their consequences on image quality, investigated in *in-silico* studies, can be found in Krah et al.[25]

Based on the above-mentioned detector systems, radiographic projections can be acquired to provide a two-dimensional map of mean residual range of the transmitted ions beyond the object of interest. With proper calibration scans (*e.g.* using special water or water-equivalent phantoms of known thickness), it is possible to convert such projection data into the water equivalent thickness (WET) of the imaged object. By comparing this experimental value with the extrapolated WET from the ray-tracing of the X-ray planning CT converted into SPR with the typical facility-specific and patient-independent calibration curve, it is thus possible to refine the SPR calibration for the specific imaged patient.[12,26–28] Moreover, radiographic ion images can enable a very low dose modality (*e.g.* 0.03 mGy[12]) for pre-treatment verification of the patient position. Extension to tomography with the acquisition of multiple projections at different angles and advanced image reconstruction methods, accounting for the curved most-likely path of the protons within the object,[29,30] can directly provide volumetric SPR information. Promising results were recently obtained from various groups who reported different phantom experiments mostly performed with small-scale prototypes and rotation of the sample rather than the beam. In particular,

Figure 1. Illustration of an image-guided adaptive workflow, where proton treatment plans are optimized on the reference SPR values (here called RSP, (A, D) and then recalculated on the SPR reconstructed from a low-dose pCT image (B, E, 1% of the full fluence) and from the proposed fluence-modulated approach (C, F), which restores approximately the same SPR quality as the reference image in the patient anatomy traversed by the beam, while reducing the fluence to 1% in less relevant anatomical regions. The corresponding dose–volume histograms are in the right column, showing equivalent dosimetric performances of the fluence modulated approach as the reference SPR. Figure from Dedes et al[32] SPR, stopping power ratio

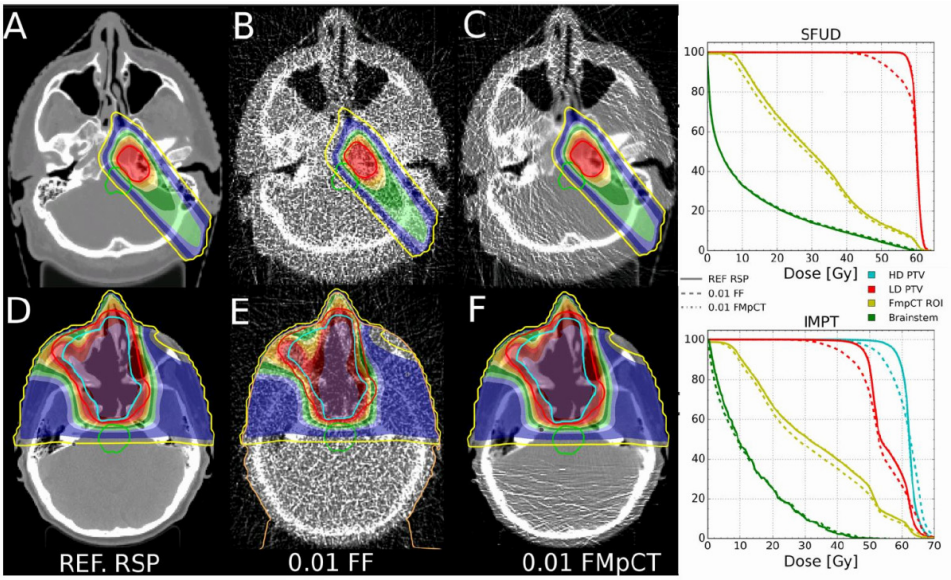

improvements in detector technology (especially with the availability of single particle tracking) and data processing (including improved estimation of the ion trajectory and energy loss estimation for the image reconstruction process) could largely overcome the limitations encountered in the first pioneering investigations of the last century and mitigate remaining issues of image reconstruction artifacts. Very recently, a second generation pCT prototype tailored to cranial anatomical locations was shown able to produce phantom images at slightly improved SPR accuracy (mean absolute percentage error, of 0.55%) compared to a state-of-the-art DECT scanner with optimal spectral separation (dual source scanner, mean absolute percentage error of 0.67%) and with a much lower imaging dose of only 1.5 mGy.[31] Further possibilities of dose reduction without compromises in image quality in anatomical regions of interest to be traversed by the beam could be achieved in imaging setups utilizing PBS, by exploiting its unique flexibility to modulate the proton fluence (Figure 1).[32] Furthermore, very recent studies suggest that the usage of the plateau region of the Bragg curve could result in biologically less harmful radiation exposure of the healthy tissue, in comparison to the low energy X-rays used for imaging.[33] Hence, ion transmission imaging promises further dosimetric benefits compared to X-ray radiation, opening new perspectives of daily image guidance at the treatment isocenter for adaptive treatment schemes.

IN-VIVO RANGE (DOSE) VERIFICATION

Despite the prospects of advanced pre-treatment imaging to provide an updated volumetric patient model with accurate SPR estimation before every treatment fraction, it would be still desirable to monitor and document the actual treatment delivery. This should ideally happen in real-time, to enable prompt interruption of a faulty beam delivery or at least compensation of errors in subsequent treatment fractions (when available). To this end, the most widely investigated monitoring techniques based on energetic photons ensuing from irradiation-induced nuclear interaction will be reviewed in the following.

Positron emission tomography

Starting from the initial proposition and early investigations in the late 1960s,[34–36] PET still represents the only clinically available method for a 3D, non-invasive, *in-vivo* monitoring of the delivered ion treatment and, in particular, of the ion beam range in the patient. This unconventional application of a meanwhile well-established nuclear medicine technique exploits the production of β^+-active target fragments (*e.g.* ^{15}O and ^{11}C with half-lives of approximately 2 and 20 min) in nuclear interactions between the incoming protons and the irradiated tissue. The ensuing signal of coincident 511 keV photons, resulting from annihilation of the positron emitted in the β^+-decay, can be acquired during or immediately after irradiation by means of customized detectors fully integrated in the dose delivery (in-beam,[37] and on-board[38]), or shortly/late after irradiation using conventional PET scanners located inside/nearby the treatment room, respectively.[39–41] Especially the in-beam approach is the most appealing but demanding solution, promising an almost real-time monitoring. To this end, geometrical constraints between the beam, patient couch and other medical equipment need to be accounted for, typically resulting in unconventional imaging geometries such as dual-head scanners[37,42] and slanted or axially shifted full rings,[43,44] which all challenge the image reconstruction process. Moreover, depending on the macroscopically

continuous (cyclotron) or pulsed (synchrotron) irradiation, higher demands are put on the data acquisition, in order to reject or at least suppress the large radiation background (*e.g.* from prompt γ, see the next section) during the actual beam-on.[45,46] On the other hand, the in-beam workflow prevents unnecessary loss of information in the time elapsed between irradiation and imaging, due to physical decay (especially of relevant short-lived emitters such as ^{15}O) as well as loss of correlation to the original place of activity production, caused by physiological washout processes such as diffusion and perfusion.[36,40] Moreover, it overcomes additional uncertainties due to possible changes of the patient position, especially when the patient is moved between treatment and imaging.

Due to the fundamental differences between the energy deposition, mostly ascribed to Coulomb inelastic interactions of the ions with the atomic electrons, and the PET activation process in nuclear interactions between the incoming ions and the tissue nuclei, the measurable β^+-activity is correlated but not identical to the dose. Hence, treatment verification is obtained by comparing the measured PET signal with a reference, either based on a previous measurement[38] (reproducibility check) or a detailed analytical[47,48] or Monte Carlo[37,40,49] calculation (accuracy check) taking into account the treatment plan (including the same patient SPR model), the time course of irradiation and imaging, and the detector response. In addition to visual inspection and qualitative analysis, range information can be deduced from different proposed approaches for a quantitative and meanwhile automated comparison of the distal fall-offs of the measured and reference activity distributions in beam-eye-view, for selected profiles or the entire distribution.[50–53]

Already in the first reported cases especially from the early in-beam (for scanned carbon ions[37]) and on-board (for passively scattered protons[38]) experience, such a comparison enabled timely identification of patient positioning changes or interfractional anatomical variations, prompting corrective measures (*e.g.* a new CT acquisition and replanning) in a few cases.[38] For the more recent experience with in-room and offline PET(/CT) monitoring of passively scattered as well as actively scanned proton irradiation at different facilities, the quantitative range analysis showed a reproducibility typically better than 1 mm,[53,54] while an accuracy mostly limited to 1–5 mm.[40,53–57] However, the latter still unsatisfactory results mostly reflect the remaining challenges in the accuracy of the PET prediction, given the considerable uncertainties in the nuclear models and cross-section data, along with limited knowledge of the patient composition and washout processes that strongly affect the proton-induced activity distribution limited to target fragments.[40,50,55,57] Moreover, the reported results are further affected by the used suboptimal instrumentation and workflows, posing additional co-registration issues and statistical noise of the imaged weak and broad activity concentrations. Hence, improved results can be expected from better modeling using additional pre-treatment imaging information (*e.g.* from DECT or MRI for tissue classification and refined washout parameters[58,59]) and latest-generation dedicated in-beam PET scanners. In particular, clinical trials are currently ongoing with the novel dual-head PET system recently integrated in the horizontal beamline of the Centro Nazionale di Adroterapia Oncologica (CNAO, Italy), for which very promising initial results have been already reported (Figure 2).[42] The system has been designed able to provide dynamic reconstruction of the acquired events with time resolution of ca. 10 s (to collect sufficient statistics) and an average delay of 6 s between delivery and image availability. Moreover, on the long-term it should be able to detect usable signal also during the beam-on time of the pulsed irradiation. Future improvements of in-beam PET imaging performances can also be expected owing to the ongoing efforts of the medical imaging community toward ultrafast detectors with coincidence time resolution around 10 ps (https://the10ps-challenge.org/), opening the perspective of real-time imaging without the need of reconstruction, and considerably reducing imaging artifacts of unconventional limited-angle geometries.[60] Additional efforts

Figure 2. Prototype in-beam PET scanner at CNAO in measuring position (a) and corresponding dynamically reconstructed activity ((b) in colorwash, left to right: every 60 s up to the final total activity, including a decay of 30 s after irradiation end) superimposed onto the grayscale patient CT for two different proton treatment fractions (top and bottom). Adapted from Ferrero et al.[42] PET, positron emission tomography.

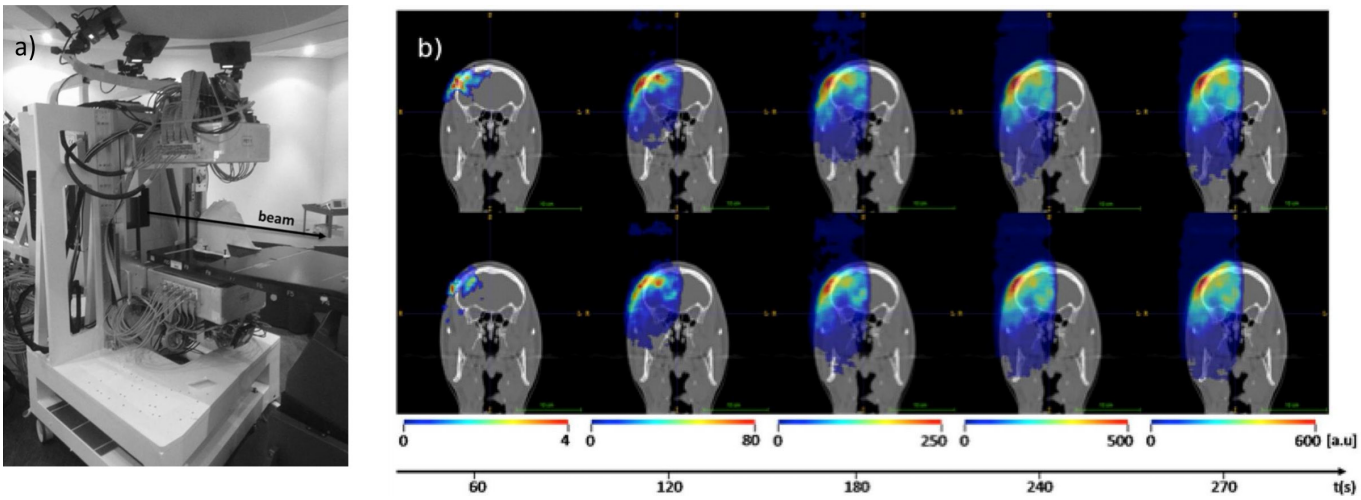

toward quasi real-time imaging aim at exploiting the signal from the very short-lived emitters such as ^{12}N, with half-lives in the millisecond range,[61] whose production is however strongly dependent on the tissue composition and whose imaging can suffer from degraded spatial resolution due to the typically high positron end point energy. Indeed, the expected advancements in image quality from optimized instrumentation and workflows in the near future will also contribute to the still outstanding goal of PET-based dose reconstruction, for which several promising approaches have been proposed,[62–64] but were so far challenged by considerable image noise and washout effects when attempted on offline acquired data.[64]

Prompt γ imaging

Initially explored in the context of the radiation background preventing acquisition of usable PET data during actual beam-on time,[65] PG radiation released from the de-excitation of tissue nuclei after nuclear inelastic interactions has been identified as a promising secondary emission for treatment verification in ion therapy.[66–68] In particular, its production almost simultaneous (within ns or less) to the irradiation can open the perspectives of a truly real-time monitoring, overcoming issues from delayed emissions and washout effects as encountered in PET imaging. However, its detection is challenged by the typically high energies of ≈2–7 MeV, characteristic for each specific nucleus, along with the additional radiation background, primarily due to neutrons. To this end, several dedicated detector developments have been proposed and pursued in the last decade, aiming to exploit different features of the PG signal such as their incoming direction, their characteristic energy and their time-of-flight.[69] As in the case of PET, range verification can be inferred from the comparison of the acquired signal with an expectation based on an analytical[70] or Monte Carlo computation,[71,72] ideally on the single pencil-beam level in beam-eye-view to provide a fast feedback during the scanned beam delivery.

The first detector solution that recently reached clinical testing is based on a knife-edge single slit collimator pointed on the distal region of interest, perpendicular to the main beam direction, to project the corresponding PG emission on a position-sensitive scintillation detector (Figure 3).[73–77] The system thus produces a one-dimensional profile along the beam path, with a fall-off even better correlated to the beam range than for PET, due to the typically lower energy threshold of the reaction cross-sections. Following the first promising deployment in passively scattered proton therapy,[75] initial clinical experience for PBS in a brain tumor indicated a Bragg-peak localization precision of around 2 mm, when aggregating the signal from nearby pencil beams to reach sufficient counting statistics (Figure 4).[73] However, this number was mostly limited by the positioning accuracy of the trolley supporting the camera (Figure 3), and improvements of the system are currently ongoing to further enhance its performance. Another full-scale system close to clinical testing combines mechanical collimation with multiple inorganic scintillator detectors of excellent energy resolution and fast timing performance, to combine the directional PG detection with their time-resolved (with respect to the accelerator radiofrequency signal) spectroscopic information to disentangle the characteristic nuclear emissions from other background radiation.[78] By using a complex Monte Carlo computational model, based on prior information of the different energy dependence of the PG yield in different materials, this approach enables extraction not

Figure 3. Schematics of the collimated PG camera projecting the PG (green lines) produced by the impinging protons (blue lines) on the position sensitive detector beyond the collimator. The upper insets depict the table-mounted U-shaped range shifter (a), the camera trolley positioning system (b) and the camera knife-edge slit collimator (c). Reprinted from Xie et al[73] with permission. PG, prompt γ.

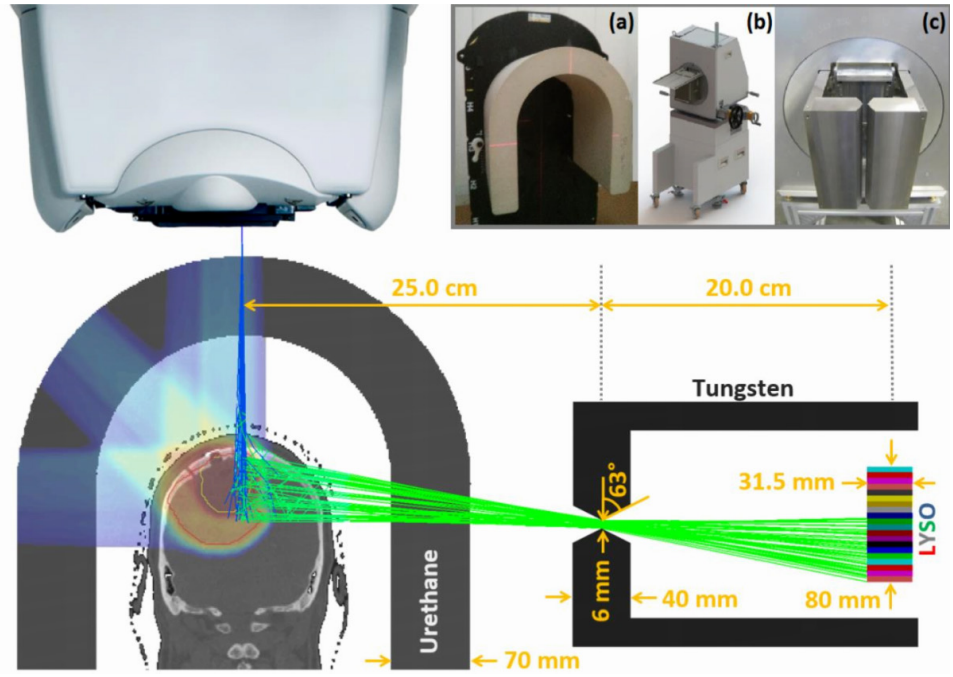

Figure 4. Exemplary PG range monitoring with the detector of Figure 3, resulting in (a) color-coded spot-by-spot range difference comparison of measurement and prediction in BEV and (b) absolute range overlaid on the patient CT from the plan (red) and the measurement (green), with aggregation. In each panel two different energy layers (top: layer #9, bottom: layer #8) of two different treatment fractions (left: fraction #21, right: fraction #23) are shown. Adapted from Xie et al[73] with permission. BEV, beam-eye-view; PG, prompt γ.

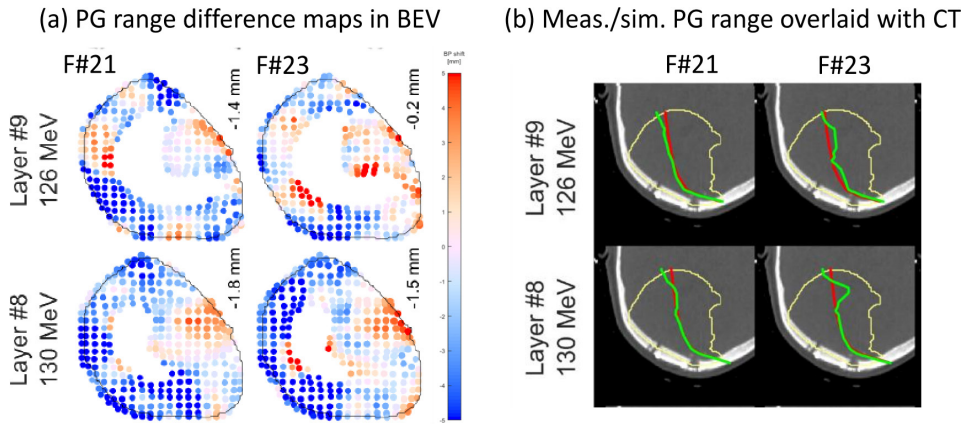

only of range information, but also of tissue composition for the main nuclei contributing to the PG signal (*e.g.* ^{12}C and ^{16}O). Promising phantom experiments at clinical doses and currents showed the potential of the system to recover the beam range with millimetre precision (at 95% confidence level) and submillimetre accuracy, again when aggregating the PG events from neighboring pencil-beam spots for improved counting statistics.[78] First intriguing attempts of dose reconstruction based on the optimal match of the computational model to the measured data were also reported. Hence, based on the promising results of the initial system characterization, a clinical trial is now underway and recruiting.

Additional solutions under research and development by different groups include the extension of the mechanical collimation concept to an increased number of photon detectors behind a multislit or multislat collimator, aiming to collect the signal emitted from the entire beam penetration depth,[79,80] or the complete removal of the massive collimation system.[81–84] The former approach would particularly enable collecting also information on the beam entrance in the patient, which might be used to detect positional or anatomical changes.[85] However, it would still suffer from the considerable reduction of counting statistics and production of secondary radiation in the collimation system. Uncollimated approaches can either exploit the time-of-flight of the detected photons with respect to a start signal coinciding with the beam transversal, mainly reflecting the range-dependent stopping time of the ions in the target, or the reconstructed Compton scattering kinematics in more complex Compton camera setups. The former so-called PG timing or peak integration method could indeed make use of very cost-effective ultrafast plastic scintillators of small footprint, but is currently still challenged by the demands of a very precise time measurement, especially with respect to the beam starting signal.[86–88] The latter approach features different flavors of multistage solid-state,[89] crystal-based[84] or thereof combination[90,91] detector arrangements, acting as scatterers or absorber. Compton camera systems indeed promise the ability of 3D imaging capabilities, but at the expense of the high complexity in the correct reconstruction of the numerous hits occurring in the detector at clinical beam currents. Among the several reported typically small-scale Compton camera systems,[69] it is worth mentioning the advanced prototype relying on commercial room-temperature semiconductor components and fully integrated in the treatment couch of a proton therapy facility.[89] Recent experimental studies with pencil beams at clinical intensities showed the system ability to produce 3D PG images and to detect range shifts in the order of 3 mm in phantoms,[92] thus bringing this technology a step forward toward clinical application.

Summarizing, PG imaging for *in-vivo* range verification of proton therapy is still a young but quite active and very promising research field, where first clinical experience is being generated with full-scale collimated camera setups, and further detector designs aiming to exploit different PG signatures are under development.

CONCLUSION AND OUTLOOK

Along with the recent improvements in beam delivery and treatment planning, in-room image guidance and *in-vivo* treatment verification are increasingly receiving attention and new impulses for research and development in proton therapy. In particular, recent progress in proton transmission imaging promises new avenues for deriving a pre-treatment patient model of improved SPR accuracy and at lower imaging doses than currently achievable with state-of-the-art X-ray imaging. In terms of *in-vivo* range verification, several secondary physical emissions are under study to provide indirect information on the actually delivered treatment and, ideally, the applied dose. Despite the often-discussed shortcomings of "delayed" emission and biological washout, PET still represents the most mature technique readily available for a 3D clinical implementation with relatively moderate efforts. Based on the encouraging clinical results obtained with suboptimal instrumentation and workflows in favorable anatomical locations like the head-and-neck, improved performances can be expected from the

latest-generation in-beam PET scanners that are just entering clinical testing, and even more intriguing perspectives of quasi-real-time imaging are given by the predicted next-generation of ultrafast PET detectors. On the other hand, even greater expectations are currently placed on methods exploiting the different PG signatures for a truly real-time range (and even dose) monitoring on a spot-by-spot basis, with first collimated systems under clinical evaluation and more detector designs under development. Additional methods not covered in this review and more specific to certain indications include the exploitation of thermoacoustic emissions induced by the localized heating of the energy deposition process, ideally co-registered with ultrasound imaging,[93,94] as well as the detection of scattered secondary protons of sufficient energy to emerge from the patient.[95] Original approaches combining different detector technologies in one single hybrid design, *e.g.* for PET and PG imaging, have also been proposed.[95,96] Indeed, the ultimate precision achievable with all these methods will considerably depend on the collected signal statistics under clinical conditions, thus calling for dedicated detector designs of high sensitivity. Moreover, the accuracy of the calculation models used to provide the reference signal to be compared to the measurement is also crucial to the final evaluation, thus calling for extensive experimental campaigns and model development. In this effort, a closer link between such calculation engines and the treatment planning system is highly desirable, as currently achieved with the computational approaches proposed in[48,97,98] for PET and PG imaging. In particular, embedding the computational engine in the treatment planning system would also enable taking considerations on statistical detectability into account at the planning stage,[99] to prevent the need of pencil-beam aggregation at least for a few critical spots, ideally identified based on the pre-treatment transmission imaging. Depending on the anatomical location, extension to time-resolved four-dimensional monitoring of motion-compensated beam delivery will also be needed and likely contribute to promoting safe treatment of moving targets. Therefore, it can be foreseen that the synergetic unconventional usage of different imaging modalities within and outside the treatment room will play a fundamental role in promoting full-clinical exploitation of the dosimetric advantages of proton beam therapy in the near future.

REFERENCES

1. Baumann M, Krause M, Overgaard J, Debus J, Bentzen SM, Daartz J, et al. Radiation oncology in the era of precision medicine. *Nat Rev Cancer* 2016; **16**: 234–49. doi: https://doi.org/10.1038/nrc.2016.18
2. Bortfeld TR, Loeffler JS. Three ways to make proton therapy affordable. *Nature* 2017; **549**: 451–3. doi: https://doi.org/10.1038/549451a
3. Schreuder AN, Shamblin J. Proton therapy delivery: what is needed in the next ten years? *Br J Radiol* 2019;: 20190359. doi: https://doi.org/10.1259/bjr.20190359
4. Nystrom H, Jensen MF, Nystrom PW. Treatment planning for proton therapy: what is needed in the next 10 years? *Br J Radiol* 2019;: 20190304. doi: https://doi.org/10.1259/bjr.20190304
5. Schneider U, Pedroni E, Lomax A. The calibration of CT Hounsfield units for radiotherapy treatment planning. *Phys Med Biol* 1996; **41**: 111–24. doi: https://doi.org/10.1088/0031-9155/41/1/009
6. Wohlfahrt P, Möhler C, Troost EGC, Greilich S, Richter C. Dual-Energy computed tomography to assess intra- and Inter-Patient tissue variability for proton treatment planning of patients with brain tumor. *Int J Radiat Oncol Biol Phys* 2019; **105**: 504–13. doi: https://doi.org/10.1016/j.ijrobp.2019.06.2529
7. Wohlfahrt P, Richter C. Status and innovations in pre-treatment CT imaging for proton therapy. *Br J Radiol* 2019;: 20190590. doi: https://doi.org/10.1259/bjr.20190590
8. Johnson RP. Review of medical radiography and tomography with proton beams. *Rep Prog Phys* 2018; **81**: 016701. doi: https://doi.org/10.1088/1361-6633/aa8b1d
9. Cormack AM. Representation of a function by its line integrals, with some radiological applications. *J Appl Phys* 1963; **34**: 2722–7. doi: https://doi.org/10.1063/1.1729798
10. Koehler AM. Proton radiography. *Science* 1968; **160**: 303–4. doi: https://doi.org/10.1126/science.160.3825.303
11. Hanson KM, Bradbury JN, Cannon TM, Hutson RL, Laubacher DB, Macek RJ, et al. Computed tomography using proton energy loss. *Phys Med Biol* 1981; **26**: 965–83. doi: https://doi.org/10.1088/0031-9155/26/6/001
12. Schneider U, Pemler P, Besserer J, Pedroni E, Lomax A, Kaser-Hotz B. Patient specific optimization of the relation between CT-hounsfield units and proton stopping power with proton radiography. *Med Phys* 2005; **32**: 195–9. doi: https://doi.org/10.1118/1.1833041
13. Schulte R, Bashkirov V, TianfangLi, ZhengrongLiang, Mueller K, Heimann J, et al. Conceptual design of a proton computed tomography system for applications in proton radiation therapy. *IEEE Trans Nucl Sci* 2004; **51**: 866–72. doi: https://doi.org/10.1109/TNS.2004.829392
14. Parodi K, Polf JC. In vivo range verification in particle therapy. *Med Phys* 2018; **45**: e1036–50. doi: https://doi.org/10.1002/mp.12960
15. Rinaldi I, Brons S, Jäkel O, et al. Investigations on novel imaging techniques for ion beam therapy: carbon ion radiography and tomography. *IEEE NSS/MIC Conference Record, MIC* 2011; 2805–10.
16. Schneider U, Besserer J, Pemler P, Dellert M, Moosburger M, Pedroni E, et al. First proton radiography of an animal patient. *Med Phys* 2004; **31**: 1046–51. doi: https://doi.org/10.1118/1.1690713
17. Poludniowski G, Allinson NM, Anaxagoras T, Esposito M, Green S, Manolopoulos S, et al. Proton-counting radiography for proton therapy: a proof of principle using CMOs APS technology. *Phys Med Biol* 2014; **59**: 2569–81. doi: https://doi.org/10.1088/0031-9155/59/11/2569
18. Bashkirov VA, Schulte RW, Hurley RF, Johnson RP, Sadrozinski HF-W, Zatserklyaniy A, et al. Novel scintillation detector design and performance for proton radiography and computed tomography. *Med Phys* 2016; **43**: 664–74. doi: https://doi.org/10.1118/1.4939255
19. Petterson M, Blumenkrantz N, Feldt J, Heimann J, Lucia D, Seiden A, et al. Proton radiography studies for proton CT. *IEEE Nuclear Science Symposium Conference Record* 2007; **2006**: 2276–80.
20. Bucciantonio M, Amaldi U, Kieffer R, Sauli F, Watts D. Development of a fast proton range radiography system for quality assurance in hadrontherapy. *Nuclear Instruments and Methods in Physics Research Section A: Accelerators, Spectrometers,*

Detectors and Associated Equipment 2013; **732**: 564–7. doi: https://doi.org/10.1016/j.nima.2013.05.110
21. Zygmanski P, Gall KP, Rabin MS, Rosenthal SJ. The measurement of proton stopping power using proton-cone-beam computed tomography. *Phys Med Biol* 2000; **45**: 511–28. doi: https://doi.org/10.1088/0031-9155/45/2/317
22. Testa M, Verburg JM, Rose M, Min CH, Tang S, Bentefour EH, et al. Proton radiography and proton computed tomography based on time-resolved dose measurements. *Phys Med Biol* 2013; **58**: 8215–33. doi: https://doi.org/10.1088/0031-9155/58/22/8215
23. Rinaldi I, Brons S, Jäkel O, Voss B, Parodi K. Experimental investigations on carbon ion scanning radiography using a range telescope. *Phys Med Biol* 2014; **59**: 3041–57. doi: https://doi.org/10.1088/0031-9155/59/12/3041
24. Farace P, Righetto R, Meijers A. Pencil beam proton radiography using a multilayer ionization chamber. *Phys Med Biol* 2016; **61**: 4078–87. doi: https://doi.org/10.1088/0031-9155/61/11/4078
25. Krah N, Khellaf F, Létang JM, Rit S, Rinaldi I. A comprehensive theoretical comparison of proton imaging set-ups in terms of spatial resolution. *Phys Med Biol* 2018; **63**: 135013. doi: https://doi.org/10.1088/1361-6560/aaca1f
26. Doolan PJ, Testa M, Sharp G, Bentefour EH, Royle G, Lu H-M. Patient-Specific stopping power calibration for proton therapy planning based on single-detector proton radiography. *Phys Med Biol* 2015; **60**: 1901–17. doi: https://doi.org/10.1088/0031-9155/60/5/1901
27. Collins-Fekete C-A, Brousmiche S, Hansen DC, Beaulieu L, Seco J. Pre-Treatment patient-specific stopping power by combining list-mode proton radiography and X-ray CT. *Phys Med Biol* 2017; **62**: 6836–52. doi: https://doi.org/10.1088/1361-6560/aa7c42
28. Krah N, Patera V, Rit S, Schiavi A, Rinaldi I. Regularised patient-specific stopping power calibration for proton therapy planning based on proton radiographic images. *Phys. Med. Biol.* 2019; **64**: 065008. doi: https://doi.org/10.1088/1361-6560/ab03db
29. Schulte RW, Penfold SN, Tafas JT, Schubert KE. A maximum likelihood proton path formalism for application in proton computed tomography. *Med Phys* 2008; **35**: 4849–56. doi: https://doi.org/10.1118/1.2986139
30. Rit S, Dedes G, Freud N, Sarrut D, Létang JM. Filtered backprojection proton CT reconstruction along most likely paths. *Med Phys* 2013; **40**: 031103. doi: https://doi.org/10.1118/1.4789589
31. Dedes G, Dickmann J, Niepel K, Wesp P, Johnson RP, Pankuch M, et al. Experimental comparison of proton CT and dual energy X-ray CT for relative stopping power estimation in proton therapy. *Phys Med Biol* 2019; **64**: 165002. doi: https://doi.org/10.1088/1361-6560/ab2b72
32. Dedes G, De Angelis L, Rit S, Hansen D, Belka C, Bashkirov V, et al. Application of fluence field modulation to proton computed tomography for proton therapy imaging. *Phys Med Biol* 2017; **62**: 6026–43. doi: https://doi.org/10.1088/1361-6560/aa7734
33. Meyer S, Kamp F, Tessonnier T, Mairani A, Belka C, Carlson DJ, et al. Dosimetric accuracy and radiobiological implications of ion computed tomography for proton therapy treatment planning. *Phys Med Biol* 2019; **64**: 125008. doi: https://doi.org/10.1088/1361-6560/ab0fdf
34. Maccabee HD, Madhvanath U, Raju MR. Tissue activation studies with alpha-particle beams. *Phys Med Biol* 1969; **14**: 213–24. doi: https://doi.org/10.1088/0031-9155/14/2/304
35. Tobias CA, Benton EV, Capp MP, Chatterjee A, Cruty MR, Henke RP. Particle radiography and autoactivation. *Int J Radiat Oncol Biol Phys* 1977; **3**: 35–44. doi: https://doi.org/10.1016/0360-3016(77)90224-3
36. Bennett GW, Archambeau JO, Archambeau BE, Meltzer JI, Wingate CL. Visualization and transport of positron emission from proton activation in vivo. *Science* 1978; **200**: 1151–3. doi: https://doi.org/10.1126/science.200.4346.1151
37. Enghardt W, Crespo P, Fiedler F, Hinz R, Parodi K, Pawelke J, et al. Charged hadron tumour therapy monitoring by means of PET. *Nuclear Instruments and Methods in Physics Research Section A: Accelerators, Spectrometers, Detectors and Associated Equipment* 2004; **525**(1-2): 284–8. doi: https://doi.org/10.1016/j.nima.2004.03.128
38. Nishio T, Miyatake A, Ogino T, Nakagawa K, Saijo N, Esumi H. The development and clinical use of a beam on-line PET system mounted on a rotating gantry Port in proton therapy. *Int J Radiat Oncol Biol Phys* 2010; **76**: 277–86. doi: https://doi.org/10.1016/j.ijrobp.2009.05.065
39. Hishikawa Y, Kagawa K, Murakami M, Sakai H, Akagi T, Abe M. Usefulness of positron-emission tomographic images after proton therapy. *Int J Radiat Oncol Biol Phys* 2002; **53**: 1388–91. doi: https://doi.org/10.1016/S0360-3016(02)02887-0
40. Parodi K, Paganetti H, Shih HA, Michaud S, Loeffler JS, DeLaney TF, et al. Bortfeld T patient study on in-vivo verification of beam delivery and range using PET/CT imaging after proton therapy. *Int J Rad Oncol Biol Phys* 2007; **68**: 920–34.
41. Zhu X, España S, Daartz J, Liebsch N, Ouyang J, Paganetti H, et al. Monitoring proton radiation therapy with in-room PET imaging. *Phys Med Biol* 2011; **56**: 4041–57. doi: https://doi.org/10.1088/0031-9155/56/13/019
42. Ferrero V, Fiorina E, Morrocchi M, Pennazio F, Baroni G, Battistoni G, Bisogni MG, et al. Online proton therapy monitoring: clinical test of a Silicon-photodetector-based in-beam PET. *Sci Rep* 2018; **8**: 4100. doi: https://doi.org/10.1038/s41598-018-22325-6
43. Crespo P, Shakirin G, Enghardt W. On the detector arrangement for in-beam PET for hadron therapy monitoring. *Phys Med Biol* 2006; **51**: 2143–63. doi: https://doi.org/10.1088/0031-9155/51/9/002
44. Tashima H, Yoshida E, Inadama N, Nishikido F, Nakajima Y, Wakizaka H, et al. Development of a small single-ring OpenPET prototype with a novel transformable architecture. *Phys Med Biol* 2016; **61**: 1795–809. doi: https://doi.org/10.1088/0031-9155/61/4/1795
45. Crespo P, Barthel T, Frais-Kölbl H, Griesmayer E, Heidel K, Parodi K, et al. Suppression of random coincidences during in-beam PET measurements. *IEEE Trans NuclSci* 2005; **52**: 980–7.
46. Sportelli G, Belcari N, Camarlinghi N, Cirrone GAP, Cuttone G, Ferretti S, et al. First full-beam PET acquisitions in proton therapy with a modular dual-head dedicated system. *Phys Med Biol* 2014; **59**: 43–60. doi: https://doi.org/10.1088/0031-9155/59/1/43
47. Miyatake A, Nishio T, Ogino T. Development of activity pencil beam algorithm using measured distribution data of positron emitter nuclei generated by proton irradiation of targets containing $^{(12)}$C, $^{(16)}$O, and $^{(40)}$Ca nuclei in preparation of clinical application. *Med Phys* 2011; **38**: 5818–29. doi: https://doi.org/10.1118/1.3641829
48. Frey K, Bauer J, Unholtz D, Kurz C, Krämer M, Bortfeld T, et al. $TPS_{(PET)}$-A TPS-based approach for *in vivo* dose verification with $_{PET}$ in proton therapy. *Phys Med Biol* 2014; **59**: 1–21. doi: https://doi.org/10.1088/0031-9155/59/1/1
49. Kraan AC. Range verification methods in particle therapy: underlying physics and Monte Carlo modeling. *Front Oncol* 2015; **5**: 150. doi: https://doi.org/10.3389/fonc.2015.00150
50. Knopf A, Parodi K, Bortfeld T, Shih HA, Paganetti H. Systematic analysis of biological and physical limitations of proton beam range verification with offline PET/CT scans.

Phys Med Biol 2009; **54**: 4477–95. doi: https://doi.org/10.1088/0031-9155/54/14/008
51. Helmbrecht S, Santiago A, Enghardt W, Kuess P, Fiedler F. On the feasibility of automatic detection of range deviations from in-beam PET data. *Phys Med Biol* 2012; **57**: 1387–97. doi: https://doi.org/10.1088/0031-9155/57/5/1387
52. Kuess P, Helmbrecht S, Fiedler F, Birkfellner W, Enghardt W, Hopfgartner J, et al. Automated evaluation of setup errors in carbon ion therapy using PET: feasibility study. *Med Phys* 2013; **40**: 121718. doi: https://doi.org/10.1118/1.4829595
53. Frey K, Unholtz D, Bauer J, Debus J, Min CH, Bortfeld T, et al. Automation and uncertainty analysis of a method for *in-vivo* range verification in particle therapy. *Phys Med Biol* 2014; **59**: 5903–19. doi: https://doi.org/10.1088/0031-9155/59/19/5903
54. Nischwitz SP, Bauer J, Welzel T, Rief H, Jäkel O, Haberer T, et al. Clinical implementation and range evaluation of in vivo PET dosimetry for particle irradiation in patients with primary glioma. *Radiother Oncol* 2015; **115**: 179–85. doi: https://doi.org/10.1016/j.radonc.2015.03.022
55. Knopf A-C, Parodi K, Paganetti H, Bortfeld T, Daartz J, Engelsman M, et al. Accuracy of proton beam range verification using post-treatment positron emission tomography/computed tomography as function of treatment site. *Int J Radiat Oncol Biol Phys* 2011; **79**: 297–304. doi: https://doi.org/10.1016/j.ijrobp.2010.02.017
56. Min CH, Zhu X, Winey BA, Grogg K, Testa M, El Fakhri G, et al. Clinical application of in-room positron emission tomography for in vivo treatment monitoring in proton radiation therapy. *Int J Radiat Oncol Biol Phys* 2013; **86**: 183–9. doi: https://doi.org/10.1016/j.ijrobp.2012.12.010
57. Handrack J, Tessonnier T, Chen W, Liebl J, Debus J, Bauer J, et al. Sensitivity of post treatment positron emission tomography/computed tomography to detect inter-fractional range variations in scanned ion beam therapy. *Acta Oncol* 2017; **56**: 1451–8. doi: https://doi.org/10.1080/0284186X.2017.1348628
58. Berndt B, Landry G, Schwarz F, Tessonnier T, Kamp F, Dedes G, et al. Application of single- and dual-energy CT brain tissue segmentation to PET monitoring of proton therapy. *Phys Med Biol* 2017; **62**: 2427–48. doi: https://doi.org/10.1088/1361-6560/aa5f9f
59. Bauer J, Chen W, Nischwitz S, Liebl J, Rieken S, Welzel T, et al. Improving the modelling of irradiation-induced brain activation for in vivo PET verification of proton therapy. *Radiother Oncol* 2018; **128**: 101–8. doi: https://doi.org/10.1016/j.radonc.2018.01.016
60. Crespo P, Shakirin G, Fiedler F, Enghardt W, Wagner A. Direct time-of-flight for quantitative, real-time in-beam PET: a concept and feasibility study. *Phys Med Biol* 2007; **52**: 6795–811. doi: https://doi.org/10.1088/0031-9155/52/23/002
61. Buitenhuis HJT, Diblen F, Brzezinski KW, Brandenburg S, Dendooven P. Beam-on imaging of short-lived positron emitters during proton therapy. *Phys Med Biol* 2017; **62**: 4654–72. doi: https://doi.org/10.1088/1361-6560/aa6b8c
62. Fourkal E, Fan J, Veltchev I. Absolute dose reconstruction in proton therapy using PET imaging modality: feasibility study. *Phys Med Biol* 2009; **54**: N217–28. doi: https://doi.org/10.1088/0031-9155/54/11/N02
63. Inaniwa T, Kohno T, Yamagata F, Tomitani T, Sato S, Kanazawa M, et al. Maximum likelihood estimation of proton irradiated field and deposited dose distribution. *Med Phys* 2007; **34**: 1684–92. doi: https://doi.org/10.1118/1.2712572
64. Remmele S, Hesser J, Paganetti H, Bortfeld T. A deconvolution approach for PET-based dose reconstruction in proton radiotherapy. *Phys Med Biol* 2011; **56**: 7601–19. doi: https://doi.org/10.1088/0031-9155/56/23/017
65. Parodi K, Crespo P, Eickhoff H, Haberer T, Pawelke J, Schardt D, et al. Random coincidences during in-beam PET measurements at microbunched therapeutic ion beams. *Nuclear Instruments and Methods in Physics Research Section A: Accelerators, Spectrometers, Detectors and Associated Equipment* 2005; **545**(1-2): 446–58. doi: https://doi.org/10.1016/j.nima.2005.02.002
66. Stichelbaut F, Jongen Y. Verification of the proton beams position in the patient by the detection of prompt gamma-rays emission. In: *39th Meeting of the Particle Therapy Co-Operative*. San Francisco, CA: Group; 2003.
67. Min C-H, Kim CH, Youn M-Y, Kim J-W. Prompt gamma measurements for locating the dose falloff region in the proton therapy. *Appl Phys Lett* 2006; **89**: 183517–3. doi: https://doi.org/10.1063/1.2378561
68. Testa E, Bajard M, Chevallier M, Dauvergne D, Le Foulher F, Freud N, Poizat JC, et al. Monitoring the Bragg peak location of 73MeV/u carbon ions by means of prompt γ-ray measurements. *Appl Phys Lett* 2008; **93**: 093506. doi: https://doi.org/10.1063/1.2975841
69. Krimmer J, Dauvergne D, Létang JM, Testa É.. Prompt-gamma monitoring in hadrontherapy: a review. *Nuclear Instruments and Methods in Physics Research Section A: Accelerators, Spectrometers, Detectors and Associated Equipment* 2018; **878**: 58–73. doi: https://doi.org/10.1016/j.nima.2017.07.063
70. Sterpin E, Janssens G, Smeets J, Stappen FV, Prieels D, Priegnitz M, et al. Analytical computation of prompt gamma ray emission and detection for proton range verification. *Phys Med Biol* 2015; **60**: 4915–46. doi: https://doi.org/10.1088/0031-9155/60/12/4915
71. Moteabbed M, España S, Paganetti H. Monte Carlo patient study on the comparison of prompt gamma and PET imaging for range verification in proton therapy. *Phys Med Biol* 2011; **56**: 1063–82. doi: https://doi.org/10.1088/0031-9155/56/4/012
72. El Kanawati W, Létang JM, Dauvergne D, Pinto M, Sarrut D, Testa É, et al. Monte Carlo simulation of prompt γ -ray emission in proton therapy using a specific track length estimator. *Phys Med Biol* 2015; **60**: 8067–86. doi: https://doi.org/10.1088/0031-9155/60/20/8067
73. Xie Y, Bentefour EH, Janssens G, Smeets J, Vander Stappen F, Hotoiu L, et al. Prompt Gamma Imaging for In Vivo Range Verification of Pencil Beam Scanning Proton Therapy. *Int J Radiat Oncol Biol Phys* 2017; **99**: 210–8. doi: https://doi.org/10.1016/j.ijrobp.2017.04.027
74. Smeets J, Roellinghoff F, Prieels D, Stichelbaut F, Benilov A, Busca P, et al. Prompt gamma imaging with a slit camera for real-time range control in proton therapy. *Phys Med Biol* 2012; **57**: 3371–405. doi: https://doi.org/10.1088/0031-9155/57/11/3371
75. Richter C, Pausch G, Barczyk S, Priegnitz M, Keitz I, Thiele J, et al. First clinical application of a prompt gamma based in vivo proton range verification system. *Radiotherapy and Oncology* 2016; **118**: 232–7. doi: https://doi.org/10.1016/j.radonc.2016.01.004
76. Priegnitz M, Barczyk S, Nenoff L, Golnik C, Keitz I, Werner T, et al. Towards clinical application: prompt gamma imaging of passively scattered proton fields with a knife-edge slit camera. *Phys Med Biol* 2016; **61**: 7881–905. doi: https://doi.org/10.1088/0031-9155/61/22/7881
77. Nenoff L, Priegnitz M, Janssens G, Petzoldt J, Wohlfahrt P, Trezza A, et al. Sensitivity of a prompt-gamma slit-camera to detect range shifts for proton treatment verification. *Radiotherapy and Oncology* 2017; **125**: 534–40. doi: https://doi.org/10.1016/j.radonc.2017.10.013
78. Hueso-González F, Rabe M, Ruggieri TA, Bortfeld T, Verburg JM. A full-scale clinical prototype for proton range verification using prompt gamma-ray spectroscopy. *Phys. Med.*

Biol. 2018; **63**: 185019. doi: https://doi.org/10.1088/1361-6560/aad513
79. Pinto M, Dauvergne D, Freud N, Krimmer J, Letang JM, Ray C, et al. Design optimisation of a TOF-based collimated camera prototype for online hadrontherapy monitoring. *Phys Med Biol* 2014; **59**: 7653–74. doi: https://doi.org/10.1088/0031-9155/59/24/7653
80. Cambraia Lopes P, Crespo P, Simões H, Ferreira Marques R, Parodi K, Schaart DR. Simulation of proton range monitoring in an anthropomorphic phantom using multi-slat collimators and time-of-flight detection of prompt-gamma quanta. *Physica Medica* 2018; **54**: 1–14. doi: https://doi.org/10.1016/j.ejmp.2018.09.001
81. Golnik C, Hueso-González F, Müller A, Dendooven P, Enghardt W, Fiedler F, et al. Range assessment in particle therapy based on prompt γ -ray timing measurements. *Phys Med Biol* 2014; **59**: 5399–422. doi: https://doi.org/10.1088/0031-9155/59/18/5399
82. Krimmer J, Angellier G, Balleyguier L, Dauvergne D, Freud N, Hérault J, et al. A cost-effective monitoring technique in particle therapy via uncollimated prompt gamma peak integration. *Appl Phys Lett* 2017; **110**: 154102. doi: https://doi.org/10.1063/1.4980103
83. Peterson SW, Robertson D, Polf J. Optimizing a three-stage Compton camera for measuring prompt gamma rays emitted during proton radiotherapy. *Phys Med Biol* 2010; **55**: 6841–56. doi: https://doi.org/10.1088/0031-9155/55/22/015
84. Llosá G, Barrio J, Cabello J, Crespo A, Lacasta C, Rafecas M, et al. Detector characterization and first coincidence tests of a Compton telescope based on LaBr3 crystals and SiPMs. *Nuclear Instruments and Methods in Physics Research Section A: Accelerators, Spectrometers, Detectors and Associated Equipment* 2012; **695**: 105–8. doi: https://doi.org/10.1016/j.nima.2011.11.041
85. Schmid S, Landry G, Thieke C, Verhaegen F, Ganswindt U, Belka C, et al. Monte Carlo study on the sensitivity of prompt gamma imaging to proton range variations due to interfractional changes in prostate cancer patients. *Phys Med Biol* 2015; **60**: 9329–47. doi: https://doi.org/10.1088/0031-9155/60/24/9329
86. Hueso-González F, Enghardt W, Fiedler F, Golnik C, Janssens G, Petzoldt J, et al. First test of the prompt gamma ray timing method with heterogeneous targets at a clinical proton therapy facility. *Phys Med Biol* 2015; **60**: 6247–72. doi: https://doi.org/10.1088/0031-9155/60/16/6247
87. Pausch G, Petzoldt J, Berthel M, Enghardt W, Fiedler F, Golnik C, et al. Scintillator-Based High-Throughput Fast Timing Spectroscopy for Real-Time Range Verification in Particle Therapy. *IEEE Trans Nucl Sci* 2016; **63**: 664–72. doi: https://doi.org/10.1109/TNS.2016.2527822
88. Werner T, Berthold J, Hueso-González F, Koegler T, Petzoldt J, Roemer K, et al. Processing of prompt gamma-ray timing data for proton range measurements at a clinical beam delivery. *Phys. Med. Biol.* 2019; **64**: 105023. doi: https://doi.org/10.1088/1361-6560/ab176d
89. Polf JC, Avery S, Mackin DS, Beddar S. Imaging of prompt gamma rays emitted during delivery of clinical proton beams with a Compton camera: feasibility studies for range verification. *Phys Med Biol* 2015; **60**: 7085–99. doi: https://doi.org/10.1088/0031-9155/60/18/7085
90. Hueso-Gonzalez F, Golnik C, Berthel M, Dreyer A, Enghardt W, Fiedler F, et al. Test of Compton camera components for prompt gamma imaging at the Elbe. *bremsstrahlung beam J Instrum* 2014; **9**.
91. Thirolf PG, Aldawood S, Böhmer M, Bortfeldt J, Castelhano I, Dedes G, et al. Development of a Compton camera prototype for medical imaging. *EPJ Web of Conferences* 2016; **117**: 05005.
92. Draeger E, Mackin D, Peterson S, Chen H, Avery S, Beddar S, et al. 3D prompt gamma imaging for proton beam range verification. *Phys. Med. Biol.* 2018; **63**: 035019. doi: https://doi.org/10.1088/1361-6560/aaa203
93. Lehrack S, Assmann W, Bertrand D, Henrotin S, Herault J, Heymans V, et al. Submillimeter ionoacoustic range determination for protons in water at a clinical synchrocyclotron. *Phys. Med. Biol.* 2017; **62**: L20–30. doi: https://doi.org/10.1088/1361-6560/aa81f8
94. Jones KC, Nie W, Chu JCH, Turian JV, Kassaee A, Sehgal CM, et al. Acoustic-based proton range verification in heterogeneous tissue: simulation studies. *Phys. Med. Biol.* 2018; **63**: 025018. doi: https://doi.org/10.1088/1361-6560/aa9d16
95. Traini G, Mattei I, Battistoni G, Bisogni MG, De Simoni M, Dong Y, et al. Review and performance of the dose Profiler, a particle therapy treatments online monitor. *Physica Medica* 2019; **65**: 84–93. doi: https://doi.org/10.1016/j.ejmp.2019.07.010
96. Parodi K. On- and off-line monitoring of ion beam treatment. *Nuclear Instruments and Methods in Physics Research Section A: Accelerators, Spectrometers, Detectors and Associated Equipment* 2016; **809**: 113–9. doi: https://doi.org/10.1016/j.nima.2015.06.056
97. Parodi K, Bortfeld T. A filtering approach based on Gaussian–powerlaw convolutions for local PET verification of proton radiotherapy. *Phys Med Biol* 2006; **51**: 1991–2009. doi: https://doi.org/10.1088/0031-9155/51/8/003
98. Pinto M, Kröniger K, Bauer J, Debus J, Dedes G, Herzog M, et al. An approach for fast estimation of positron-emitter and prompt-gamma distributions in RayStation for proton therapy monitoring. *International Conference on the Use of Computers in Radiation Therapy* 2016;: 27–30.
99. Tian L, Landry G, Dedes G, Kamp F, Pinto M, Niepel K, et al. Toward a new treatment planning approach accounting for *in vivo* proton range verification. *Phys. Med. Biol.* 2018; **63**: 215025. doi: https://doi.org/10.1088/1361-6560/aae749